IPPI
Polyolefins Journal, Vol. 11, No. 3 (2024)
DOI: 10.22063/POJ.2024.3606.1304
ORIGINAL PAPER

Correlation of morphology, rheology, and impact strength in compatibilized polypropylene/ polybutadiene rubber thermoplastic vulcanizates

Somayeh Rafiei[1], Davood Soudbar[2,*], Minoo Sadri[3], Fatemeh Shafiei[1]

[1]Department of Chemistry, Arak Branch, Islamic Azad University, Arak, Iran
[2]Research and Development Department of Shazand Petrochemical Co., Arak, Iran
[3]Faculty of Chemistry and Chemical Engineering, Malek Ashtar University of Technology, Tehran, Iran

Received: 13 April 2024, Accepted: 23 April 2024

ABSTRACT

Thermoplastic vulcanizates (TPVs) were prepared based on polypropylene (PP) and polybutadiene rubber (PBR) at different PP/PBR compositions (70/30 and 60/40). PP-grafted-maleic anhydride (PP-*g*-MA) was introduced into the TPVs at different concentrations (10 and 20%). The compatibilizing effect of PP-*g*-MA was demonstrated through cross-sectional morphology. PP-*g*-MA exhibited a suppressing impact on the coalescence of the rubber domains, leading to a finer and more uniform distribution of the PBR phase. Due to the higher rubber content, the compatibilizing effect was more pronounced for the 60/40 composition, which was on the verge of forming a co-continuous morphology. However, it was found that a higher PP-g-MA content is needed to effectively compatibilize the TPVs. Rheological results revealed opposing effects on the viscoelastic response of the system. However, the elastic response was intensified once higher content of PP-*g*-MA was used, suggesting its compatibilizing role. Dynamic mechanical analysis results proved the existence of opposing effects and revealed the profound compatibilizing effects of PP-*g*-MA, especially at higher content (20%). Izod impact strength exhibited moderate and notable enhancements in both TPV compositions by adding 10% and 20% of PP-*g*-MA, respectively, attributed to the highly increased compatibility of the PP/PBR TPVs, especially at higher levels of PP-*g*-MA content. **Polyolefins J (2024) 11: 137-148**

Keywords: Polypropylene; polybutadiene rubber; thermoplastic vulcanizates; impact strength; morphology.

INTRODUCTION

Thermoplastic vulcanizates (TPVs) are polymer blends with interesting properties since they simultaneously present the mechanical properties of a cross-linked elastomer and the good processability of a thermoplastic [1]. In the mixing process, the elastomer phase is cross-linked, which leads to a polymer phase inversion due to the considerable change in the viscoelastic response of the elastomer. TPVs have gained tremendous attention, especially in the electronics, building, and automotive industries, due to their excellent mechanical properties, high elasticity, and suitable processability [2]. Above their glass transition temperature (T_g), TPVs act as a thermoplastic polymer and can be melted above their melting point (T_m). Therefore, traditional plastic processing methods, such as extrusion and injection molding, can be employed to manufacture TPVs.

Due to its good physical and mechanical properties and processability, polypropylene (PP) has been utilized in numerous applications [3-6]. One of PP's major drawbacks is its poor impact strength, which

*Corresponding Author - E-mail: soudbar.d@gmail.com

CC BY NC SA

has been the reason for blending it with rubbers and producing thermoplastic elastomers [7,8]. In one study, EPDM was added to the PP phase to produce TPVs with increased mechanical properties for automotive applications [9]. Polybutadiene rubber (PBR) is a proper candidate to be added to PP and produce high-quality TPV materials due to its excellent elasticity, good wear resistance, and low price [10,11]. PBR exhibits a higher wear resistance and lower rolling resistance than styrene-butadiene rubber and natural rubber due to its lower glass transition temperature (~ -100°C) [12,13]. Therefore, PP/PBR blends possess a promising potential to produce TPVs commercially. However, their large-scale production has been limited by the high level of incompatibility between the elastomeric and plastic phases, which triggers the phase separation process [14]. Such a high incompatibility in PP/PBR TPVs leads to an unstable morphology, even though both PP and PBR polymers are nonpolar. Therefore, to increase the potential of PP/PBR TPVs for large-scale production, their compatibility level should be enhanced. It is well-established that compatibilizers play a key role in homogenizing the mixtures and achieving the desired properties [15-19]. In the case of PP/rubber blends, one effective method is to increase their compatibility via incorporating a proper compatibilizer [20-24]. Saiwari et al. [20] demonstrated the potential of maleic anhydride to compatibilize TPVs based on PP and recycled rubber. In another study, an epoxidized natural rubber/maleic anhydride-grafted polypropylene blend was utilized as a compatibilizing agent for PP/NR blends [23]. In one of the few studies on PP/PBR systems, Sheng et al. [25] have used an acrylate-modified PBR to compatibilize the PP/PBR blends, which resulted in a notable reduction in the size of the PBR phase. In another study, in-situ compatibilization was employed to compatibilize PP/PBR blends [26]. In the current research, we produced PP/PBR thermoplastic vulcanizates via a melt-mixing method and used polypropylene-grafted-maleic anhydride (PP-*g*-MA) as a compatibilizing agent. The effects of different compatibilizer contents and blend ratios on morphological, rheological, and dynamic mechanical properties were also studied.

Table 1. List of the prepared samples and their coding.

Samples	PP (wt.%)	PBR (wt.%)	PP-g-MA (% w/w)
PP	100	-	-
P7B3	70	30	-
P7B3-10	70	30	10
P7B3-20	70	30	20
P6B4	60	40	-
P6B4-10	60	40	10
P6B4-20	60	40	20

EXPERIMENTAL

Materials

Polypropylene (PP), with a melt flow index of 0.3 g/10 min, and polybutadiene rubber, with cis content of 97%, were supplied from the Shazand Petrochemical Company (Arak, Iran). Stearic acid (Wilfarin SA-1865) (Wilfarin Company, India) and zinc oxide (Sigma-Aldrich, USA) were used as activator of sulfur vulcanization. The employed processing aid for PBR masterbatch was paraffinic oil and supplied by Behran Oil Company (Iran). The vulcanization accelerator was N-tert-butyl-2-benzothiazyl sulfenamide (TBBS) and supplied from Jing Xian Yuelong Company (China).

Samples preparation

PBR and PP granules were first dried at 80°C for 16 h. A masterbatch was prepared using PBR, stearic acid, zinc oxide, and paraffinic oil. After roll-milling, it was mixed with various amounts of PP to obtain 30/70 and 40/60 PBR/PP compositions. The selected blend ratios were based on the preliminary experiments, which revealed their better mechanical properties. The temperature of the melt-mixing process was 180°C, and the rotor speed was 60 rpm. The PBR masterbatch was first mixed for 10 minutes and then mixed with PP for 5 minutes. Sulfur, as the curing agent, was added to the mixture along with TBBS as an accelerator. Once a curing peak appeared in the torque-time curve, the mixing process continued for another 10 minutes. Finally, the mixtures were molded under a pressure of 15 MPa at 180°C to prepare the sheets. The formulation of prepared samples is reported in Table 1.

Characterization.

Scanning electron microscopy (SEM) coupled with energy-dispersive X-ray (EDX) spectroscopy (VEGA//TESCAN instrument, Czech Republic) was employed to evaluate the cross-sectional morphology of the prepared samples at the voltage of 25 kV. To this end, the samples were cryogenically fractured in liquid nitrogen, followed by immersion in xylene to etch out the PBR phase preferentially. Before the scanning, all the samples were coated with gold to prevent any electric charging (K450; Emitech, Kent, UK). To study the rheological behavior, an

MCR300 strain-controlled rheometer (Anton Paar) was employed in oscillation mode. The parallel plate geometry, with a diameter of 25 mm, was used to conduct the experiments under a nitrogen atmosphere at 200°C. To determine the linear viscoelastic region of the samples, strain amplitude sweeps were first performed from 0.0001% to 10% at an angular frequency of 1 rad/s. After that, the frequency sweeps were conducted on the samples within the frequency range of 0.01-628 rad/s. Eventually, the steady-state shear tests were carried out at the same temperature within the shear rate range of 0.001-30 s^{-1}. Dynamic mechanical analysis (DMA) was performed on a Triton Technology DMA (TTDMA) from Tritron Technology Ltd., Keyworth, UK. Measurements of storage modulus (E') and tan δ were performed at a heating rate of 5°C/min and a frequency of 1 Hz in a strain of 0.02 mm from -120°C to 100°C. To assess the toughness of the prepared samples, the values of notched Izod impact strength were measured. A Zwick impact test instrument was used to perform the notched specimens according to the ISO 180 test procedure at room temperature for a notch tip radius of 1 mm. The impact test was repeated at least five times, and the average of the obtained results was reported.

The degree of crosslinking in the samples was assessed by measuring the gel content in accordance with ASTM D 2765. Each sample was enclosed in a cellulose bag with an accurate weight of about 0.2 g. This bag was then subjected to a 24-hour Soxhlet extraction process using p-xylene as the extracting solvent. After extraction, the bags were dried in an oven at 80°C until constant weight. The gel content was subsequently calculated using the following method [27]:

$$Gel\ content(\%) = \frac{Weight\ after\ extraction}{Initial\ weight} \times 100$$

The measurement of tensile properties was conducted using the INSTRON Universal Testing Machine, following ASTM D638 standards. This was carried out at a crosshead speed of 50 mm/min, utilizing dog-bone-shaped test specimens.

RESULTS AND DISCUSSION

The cross-sectional SEM images of the prepared samples are reported in Figure 1. All the samples' surfaces exhibited a rough surface, suggesting the occurrence of a tough fracture [28]. Also, all the samples demonstrated a very fine droplet-in-matrix morphology, with the PBR phase playing the role of the dispersed phase. In many of the rubber/plastic blend systems, the size of the rubber droplets is in the range of 0.5 to several micrometers [29]. In the traditional TPV systems, the plastic phase is first

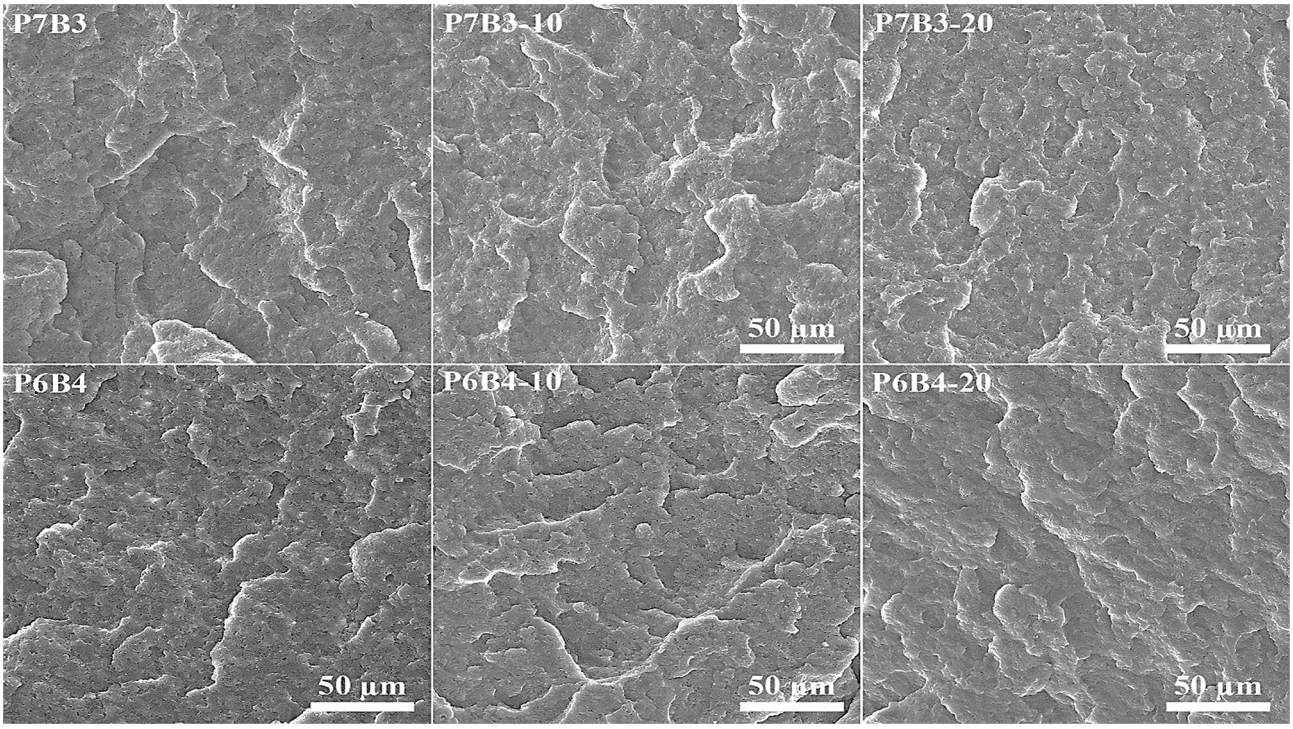


Figure 1. Cross-sectional SEM images for all the prepared samples at the magnification of 1000×.

dispersed within the rubber phase due to the high rubber content. Then, a phase inversion occurs during the dynamic vulcanization [2]. In the current research, the plastic phase contents (70 and 60%) were higher than the rubber phase contents (30 and 40%). Therefore, the rubber phase remained as the dispersed phase during the dynamic vulcanization.

To better evaluate the impact of compatibilizer content on the morphology of TPVs (70/30 blend ratio), the SEM images are reported at higher magnifications in Figure 2. The obtained results for the uncompatibilized TPV reveal that the PBR phase has been distributed at the submicron scale within the PP matrix; however, some irregular and larger domains were also formed (marked in Figure 2), which are the result of the coalescence of the finer PBR domains. Under shear stress, the rubber phase is broken up into submicron-scale droplets, followed by an inhomogeneous vulcanization process. As a result, the coalescence phenomenon may be impeded for those submicron-scaled domains with a higher crosslink density. In contrast, those submicron-scaled domains with a lower crosslink density can coalesce and form irregular rubber domains with the size of several micrometers. The main reason for the enhanced coalescence in the case of rubber domains with a low crosslink density can be ascribed to their lower viscosity and ease of chain mobility during the vulcanization process [2].

Upon the addition of 10% of PP-*g*-MA as the compatibilizer, the cross-sectional morphology became more uniform, leading to a reduced coalescence of PBR domains. As the PP-*g*-MA content increased to 20%, the morphology became more uniform, and no coalescence occurred, based on a large SEM scanning. These results imply that the addition of PP-*g*-MA has been highly influential on the compatibility level of the TPV with a blend ratio of 70/30. The observed compatibilizing effect of PP-*g*-MA can be attributed to the localization of PP-*g*-MA in the interface region, leading to improved interfacial adhesion between the TPV components [30,31].

Figure 3 shows the cross-sectional morphology of the TPVs prepared at the blend ratio of 60/40, loaded by 10 and 20% of PP-g-MA as compatibilizer. Comparing Figure 3 and Figure 2, the coalescence of PBR domains increased upon increasing the PBR content from 30 to 40 wt.%. This is the reason for the increased phase separation in the case of P6B4-10, i.e., reduced blend compatibility. However, the level of coalescence is not high enough to cause a co-continuous morphology for the TPVs at a blend ratio of 60/40. As the PP-g-MA content increased to 20%, the cross-sectional morphology became more uniform, suppressing PBR phase coalescence. This phenomenon resulted in a distribution of fine and

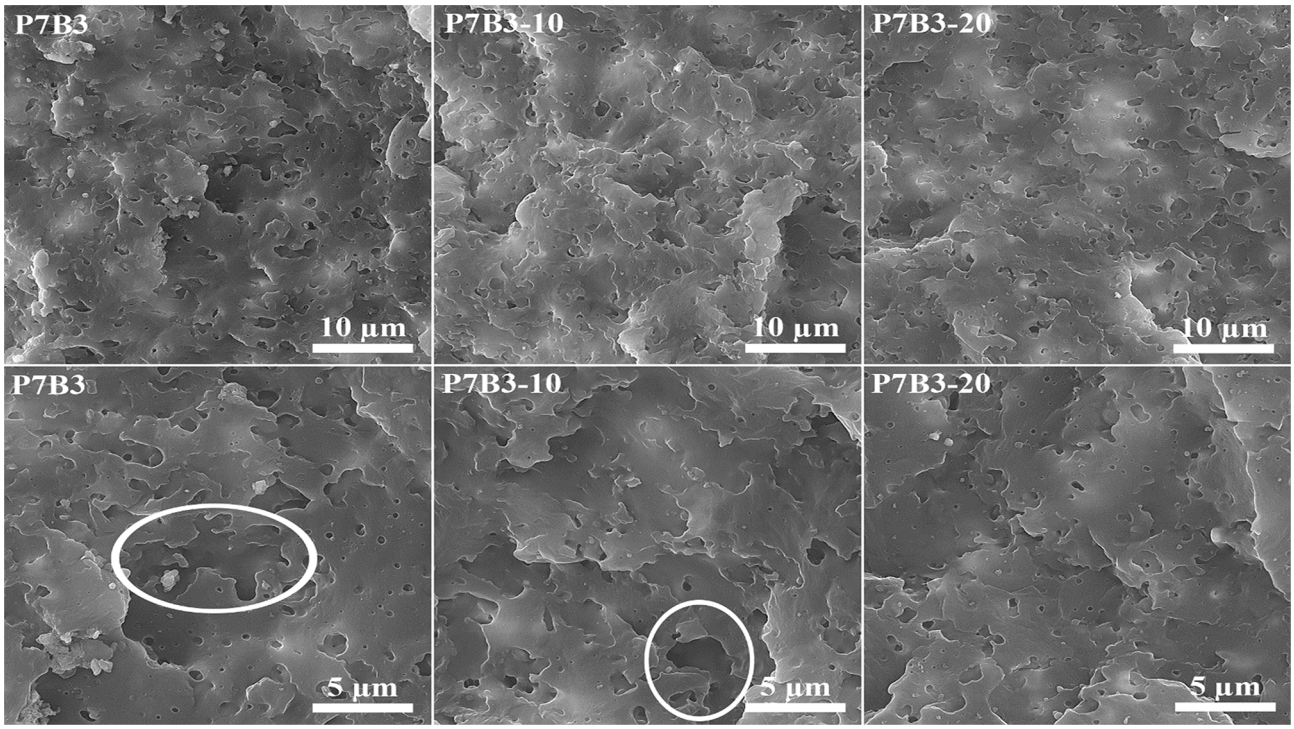


Figure 2. Effect of compatibilizer content on the cross-sectional morphology of TPVs at blend ratio of 70/30. The top and bottom row images were taken at magnifications of 5000× and 10000×.

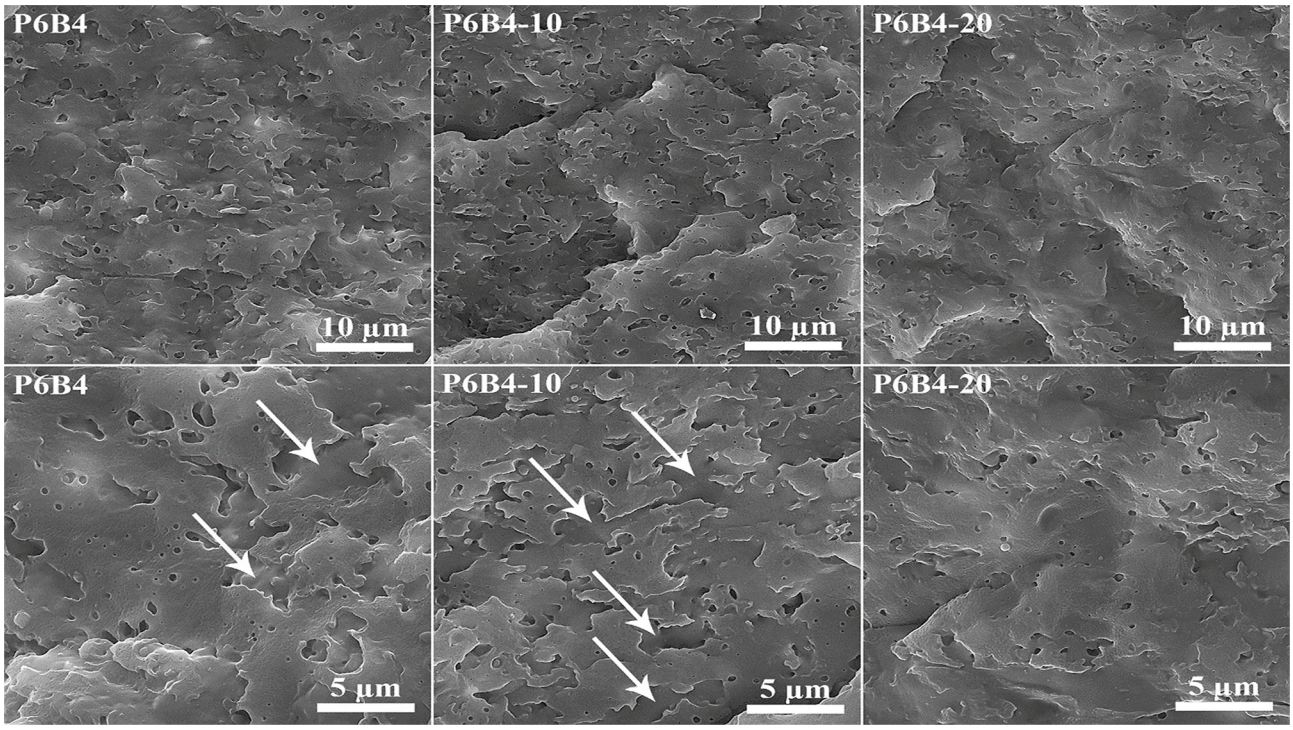


Figure 3. Effect of compatibilizer content on the cross-sectional morphology of TPVs at blend ratio of 60/40. The top and bottom row images were taken at magnifications of 5000× and 10000×.

discreet PBR domains within the PP matrix. Overall, one can conclude that the addition of PP-g-MA as a compatibilizer, especially at a concentration of 20%, results in improved compatibility between the TPV components.

Table 2 shows the gel content of the developed samples. The table clearly indicates that the gel content of the TPVs increased with the increase in the concentration of PP-g-MA. This trend could be attributed to the role of PP-g-MA as a compatibilizer. It likely facilitates better interaction and crosslinking between the PP and PBR phases. At 0% PP-g-MA, the gel content was the lowest for both compositions (40.4% for 70/30 and 51.5% for 60/40), suggesting minimal crosslinking in the absence of a compatibilizer. With 10% and 20% PP-g-MA, the gel content increased significantly, indicating enhanced crosslink density due to the compatibilizing effect.

On the other hand, the composition of PP/PBR shows a substantial impact on the gel content. For the 60/40 PP/PBR blend, the gel content was consistently higher across all levels of PP-g-MA concentration compared to the 70/30 blend. This observation could be related to the higher rubber content in the 60/40 blend, which naturally has a higher tendency to form cross-linked structures, thereby increasing the gel content. The obtained results are consistent with previous studies reported in the literature [32,33].

As it is clear, thermoplastic vulcanizates (TPVs) are dynamic vulcanizable blends that are mainly composed of fully cured unsaturated rubber particles in a polypropylene (PP) matrix. Our blend also has the same components as TPV, and positive changes in measured properties such as modulus, ultimate tensile strength, gel content, etc., indicating crosslinking and the formation of such a material.

To assess the processability and determine the viscoelastic response of the prepared TPVs, rheological properties were evaluated. At first, we needed to prove the time independency of the prepared samples, and the results are depicted in Figure 4. According to Figure 4a, which depicts the damping factor (tan δ = G''/G') versus time, the tan δ values remained nearly constant within the time period of the experiment (2 h). Another observation from time sweep results is that the tan δ curves for 60/40 blends lay notably below the curves of 70/30 blends due to the higher PBR content

Table 2. Get content of the developed sample.

Sample code	Gel content (%)
P7B3	40.4
P7B3-10	44.9
P7B3-20	53.7
P6B4	51.5
P6B4-10	59.2
P6B4-20	64.7

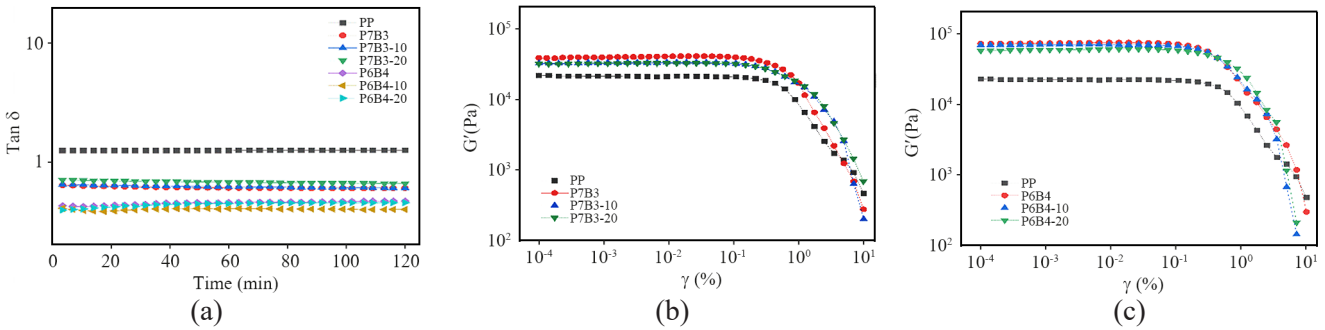


Figure 4. (a) Tan δ versus time curves obtained from the time sweep rheological experiments for all the samples. G' versus strain curves obtained from the strain sweep rheological experiments for the neat PP and TPVs at blend ratios of (b) 70/30 and (c) 60/40.

and increased system elasticity.

The variation of G' values in terms of the applied strain is illustrated in Figures 4b and 4c to determine the linear viscoelastic (LVE) region, characterized by the critical strain, γ_c, corresponding to the onset of nonlinearity. Based on Table 3, the γ_c value reduced from 0.3% for the neat PP sample to 0.25% and 0.15% for P7B3 and P6B4, respectively. Such a result is quite expected since the addition of a rubbery phase increases the complexity of the system's internal structure, leading to a shorter LVE region [31]. It was also observed that adding different contents of the compatibilizer caused no significant changes in the length of the LVE region.

The storage and loss modulus curves are depicted in Figure 5 in terms of angular frequency for the neat PP and its corresponding TPVs. In contrast to the neat PP sample, for which a dominating viscose response was detected, all the TPVs exhibit a dominating elastic response. The cross-over point, below which the viscose response dominates the rheological behavior of the neat PP samples, has disappeared for all the TPVs, implying an increased elastic response resulting from PBR addition. Based on Figure 5, the vertical difference between the G' and G'' curves became more profound in the case of 60/40 TPVs, implying a profound elastic response. It can also be stated that the G' values for all the TPVs are independent of frequency within the low-ω region, implying a pseudo-solid-like behavior for the TPV samples.

The G' curves of all the samples are compared in Figure 6a. The profound influences of PBR addition and the fabrication of thermoplastic vulcanizates on the viscoelastic response are evident. As mentioned earlier, the G' curves of all TPVs exhibit a non-terminal behavior, which can be attributed to a network structure formed by rubber particle agglomerates [34]. Figure 6a shows a notable difference between the G' curves of TPVs prepared at blend ratios of 70/30 and 60/40. The slope values of G' curves at the low-ω region (ω<0.1) are reported in Table 3. The G' curve slope was significantly decreased from 1 in the case of the neat PP sample to 0.04 and -0.01 upon incorporating 30 and 40 wt.% of PBR, respectively. The obtained negative G' slope for P6B4 can be attributed to an upturn in the G' values at the terminal region. One may infer that increasing the rubber content led to a profoundly interconnected network structure resulting from the rubber particle interactions. Since the appearance of G' upturn within the low-ω region may be associated with the formation of a co-continuous morphology [24], it can be inferred that the P6B4 sample is on the verge of forming a co-continuous morphology and adding PP-g-MA made the droplet-in-matrix more stable, preventing the change of morphology to co-continuous.

In the case of the 30/70 blend ratio, adding 10% of compatibilizer increased the G' slope from 0.04 to 0.12, indicating a decline in the elastic response of P7B3 as a result of compatibilizer incorporation. On the one hand, adding a compatibilizer increases the system flowability, which leads to increased viscose response.

Table 3. Critical strain values obtained from strain sweep and slope of G' curves obtained from frequency sweet experiments for all the samples.

Samples	PP	P7B3	P7B3-10	P7B3-20	P6B4	P6B4-10	P6B4-20
γ_c (%)	0.3	0.25	0.2	0.22	0.15	0.17	0.21
Slope of G' curve	1	0.04	0.12	0.13	-0.01	0.02	0.02

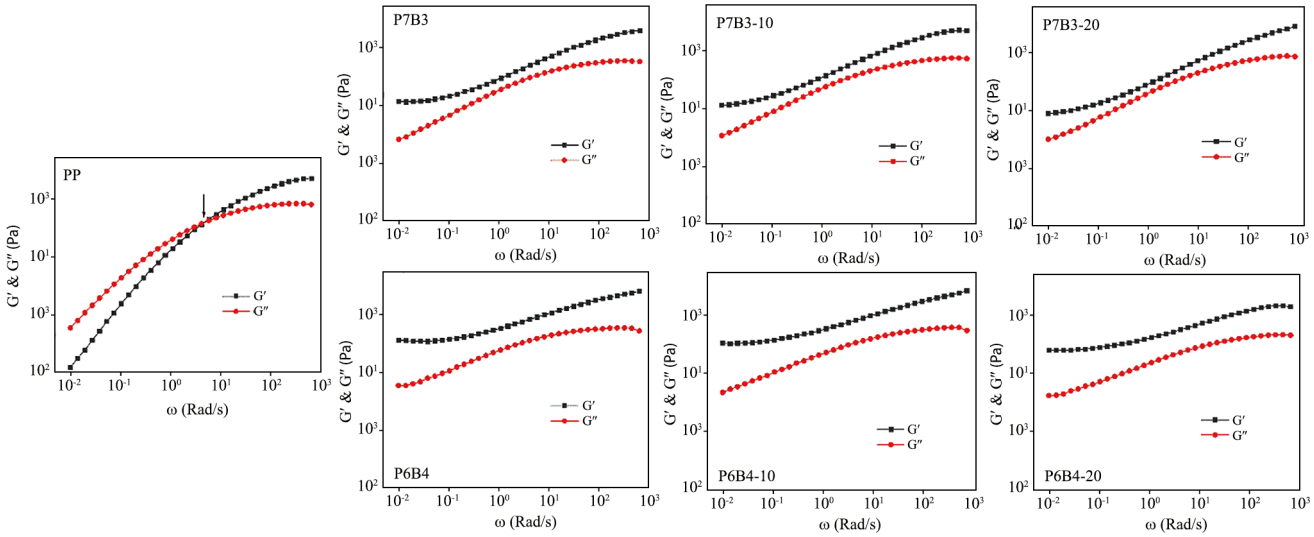


Figure 5. Storage and loss modulus curves in terms of angular frequency for all the samples.

On the other hand, the compatibilizing effect of PP-g-MA results in an increase in the elastic response due to the uniform and fine distribution of rubber domains within the plastic matrix. Considering the increased viscose behavior for P7B3-10, the former mechanism dominates upon adding 10% of compatibilizer. According to the magnified view of the low-ω region in Figure 6a, the G' curve shifted to lower values as a result of increasing the PP-g-MA content to 20%. This result can be ascribed to the induced flowability upon adding a compatibilizer, which reduces the storage modulus values within the terminal region. However, Table 3 reveals that adding 20% of PP-g-MA made no discernible changes in the slope of G' curve. The fact that adding 20% of a compatibilizer did not result in a higher G' slope value, i.e., a higher viscose response, indicates that the improved compatibility of the system might have come to play a role in the system's viscoelastic response. Therefore, one can attribute the obtained result to the enhanced elastic response of the system, as a result of better compatibility, which counterbalanced the aforementioned mechanism, leading to the same G' curve slope for P7B3-10 and P7B3-20 samples. The improved compatibility of P7B3-20 has been earlier demonstrated in Figure 2.

In the case of 60/40 TPVs, a similar trend can be seen for the G' curves within the low-ω region, according to the magnified view in Figure 6a. The addition of 10% PP-g-MA into P6B4 increased the G' slope from -0.01 to 0.02; however, further increment of compatibilizer content to 20% caused no changes in the G' slope. Similar to the 70/30 TPVs, increasing the PP-g-MA content to 20% decreased the G' values. This result can be used as a hint for the compatibilizing role of PP-g-MA at higher concentrations and conforms with the obtained SEM results.

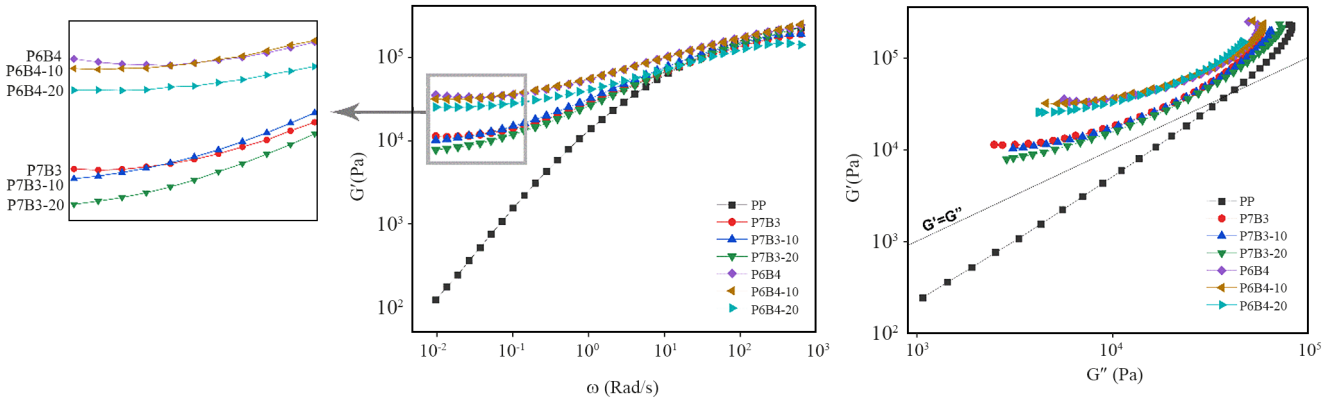


Figure 6. (a) G'-ω curves for the neat PP sample and all the prepared TPVs. The inset is a magnified view of the curves within the low-ω region. (b) Han plots for all the samples.

According to Figure 6b, which depicts the Han plots for all the samples, the only sample with a curve below the G'=G" line is the neat PP, which implies a viscose response. On the other hand, the Han plots for all the prepared TPVs lie above the G'=G" line, indicating a significant elastic behavior enhancement upon the PBR phase inclusion. The two series of prepared TPVs (70/30 and 60/40) show distinctly different curves, with the 60/40 TPVs having the most deviation from the G'=G" line. For the TPV samples, the deviation phenomenon appears within the low-ω region, and results from the phase separation in blend systems [35]. Therefore, one can infer that in both series of TPVs, inclusion of 20% of PP-g-MA as compatibilizer reduced the extent of the deviation, indicating an improved level of compatibility in the system.

Figure 7 shows the storage modulus (E') values for all the samples obtained from the dynamic mechanical analysis. According to Figure 7a, at temperatures below -90°C, which is below the glass transition region of the PBR phase, an interesting trend can be observed in E' values. It is seen that adding 10% of PP-g-MA caused a reduction in the E' values, whereas increasing its content to 20% resulted in an enhancement in the E' values even beyond the uncompatibilized TPV (P7B3). These results perfectly corroborate our findings from SEM and rheological experiments. At lower content of PP-g-MA (10%), the dominating mechanism is the induced flowability due to the low viscosity of the compatibilizer. The increased chain mobility in P7B3-10 could increase the free volume, leading to lower E' values within the glassy region. With this logic in mind, increasing the compatibilizer content is expected to decrease the E' values further. Still, as we see in Figure 7a, the E' values were notably increased in the case of P7B3-20, which are even higher than the uncompatibilized TPV. Here, the dominating mechanism is the improved compatibility between PP and PBR, which counterbalances the aforementioned mechanism. In fact, 20% of PP-g-MA has successfully led to a finely distributed PBR phase within the PP matrix, which is responsible for the enhanced elastic response. Interestingly, with the start of the glass transition region of the PBR phase (>90°C), the E' curve for P7B3-10 is first superimposed and then lies above that of P7B3. This phenomenon may be the compatibilizer's diminishing effect on the system's chain mobility as temperature increases, resulting in the domination of the compatibility improvement mechanism for P7B3-10.

According to Figure 7b, a nearly similar trend can also be observed for 60/40 TPVs. Within the glassy region, the E' values first show a reduction upon adding 10% compatibilizer and then an enhancement as the compatibilizer content increases to 20%. This is also in agreement with our previous observations from morphology and rheology results. It can be concluded that once the PP-g-MA content is 20%, the TPV compatibility is highly improved. One difference between the results of 60/40 and 70/30 TPVs is that the E' curve for P6B4-10 lies below the P6B4 curve within all the studied temperature range. Because the compatibilizing effect of PP-g-MA at 10% concentration for 60/40 TPVs is somehow weaker than that for the 70/30 TPVs. The reason for this is the higher extent of coalescence of the rubber phase for 60/40 TPVs, for which 10% of PP-g-MA is not

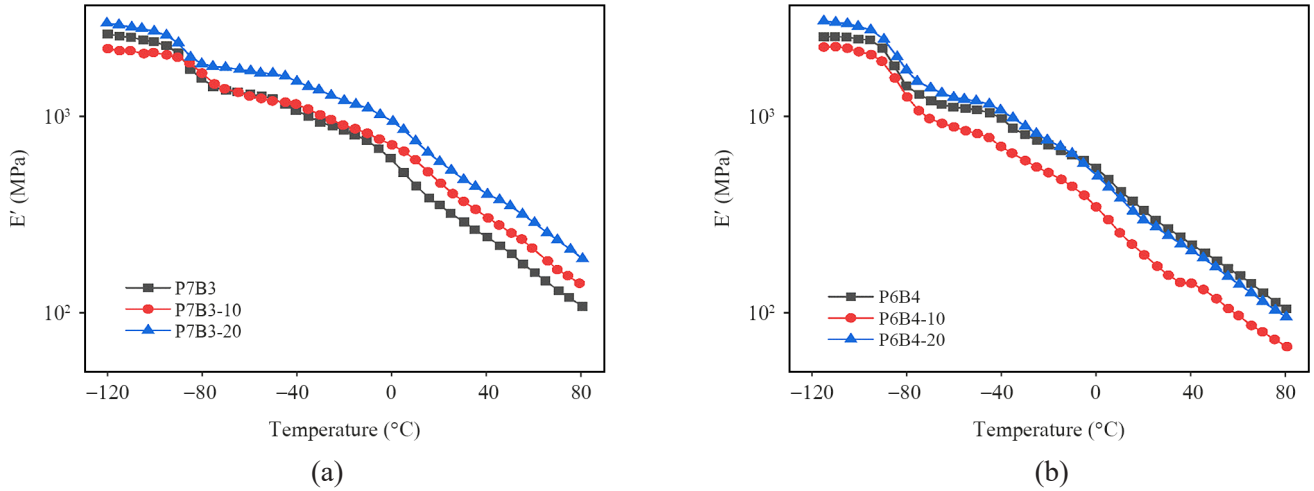


Figure 7. E' curves in terms of temperature for (a) 70/30 and (b) 60/40 TPVs.

enough to create a profound compatibilizing effect. As a result of a weaker compatibilizing effect, the viscose response has increased within all the temperature range and shifted the E' curve downward.

One of the aims of blending PP with rubbers is to improve its impact strength. In the current study, the notched Izod impact strength of the prepared samples was measured and depicted in Figure 8. It is well-established that the impact strength of plastic/rubber blends can be improved by reducing the size of the dispersed rubber phase and improving the interfacial compatibility [36,37]. In fact, the larger rubber domains may increase crack propagation at the blend interface, which leads to brittle behavior. The obtained results revealed that the impact strength increased from 5.3±0.9 kJ/m^2 for the neat PP sample to 31.2±2.2 kJ/m^2 for P7B3, exhibiting a fivefold enhancement upon the addition of 30 wt.% of PBR. During the impact test, stress concentration first occurs in the PP phase and then develops to form a crack. The PBR phase impedes the crack expansion by absorbing energy [38]. In other words, PP/PBR interface delivers the impact stress from the PP matrix to PBR domains.

Quite unexpectedly, further increment of PBR content to 40 wt.% led to an insignificant increase in the impact strength (33.1±1.9 kJ/m^2). It can be inferred that increasing the rubber concentration increases the impact strength only provided that the rubber phase distribution remains uniform with fine particle size. But the obtained SEM results earlier revealed the increased coalescence of the rubber domains at 60/40 composition, which leads to counterbalancing the effect of increased rubber concentration. Thus, no significant improvement in impact strength was obtained for P6B4. In the case of 70/30 TPVs, the addition of 10% of PP-g-MA increased the impact strength from 31.2±2.2 kJ/m^2 to 37.4±2.1 kJ/m^2, equal to ~20% enhancement. This result suggests that 10% of compatibilizer has been rather successful in reducing the coalescence of PBR domains and improving the PP/PBR compatibility, as demonstrated earlier in SEM and rheological experiments. However, as the PP-g-MA content increased to 20%, the impact strength increased significantly (47.7±1.6 kJ/m^2), indicating a 52% enhancement with respect to the uncompatibilized TPV (P7B3). This result suggests that 20% of PP-g-MA has successfully suppressed the coalescence of rubber domains and improved the PP/PBR compatibility.

In the case of 60/40 TPVs, adding 10% of PP-g-MA increased the impact strength to 37.9±1.7 kJ/m^2

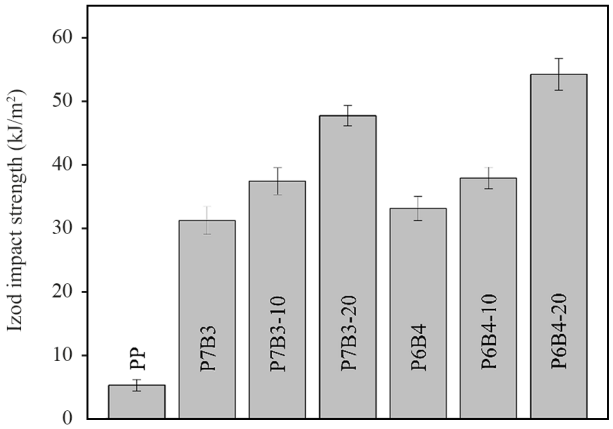


Figure 8. Izod impact strength values for all the samples.

(14% enhancement), which is lower than that for the 70/30 TPV (20% enhancement). It was previously noted that 10% of PP-g-MA is not a suitable concentration to efficiently compatibilize the 60/40 TPVs, due to the increased rubber content and the higher tendency of the PBR domains for coalescence. In contrast, increasing the PP-g-MA content to 20% significantly improved the impact strength to 54.2±2.5 kJ/m^2 (64% enhancement). Quite unexpectedly, the influence of 20% compatibilizer for the 60/40 TPV is more pronounced than that for the 70/30 TPV (64% versus 52% enhancement in impact strength). One may conclude that adding 20% of PP-g-MA deviated the system from being on the verge of co-continuity to a stable and finely distributed droplet-in-matrix morphology. This is the main reason for the considerable improvement in the impact strength of TPVs at 60/40 composition. Considering the obtained results, we may also highlight the role of the interfacial layer in stress transfer to the rubber phase, as previously noted in other works [39].

The tensile properties of polypropylene/polybutadiene rubber (PP/PBR) blends, both with and without maleic anhydride grafted polypropylene compatibilizer (PP-g-MA), were investigated to understand their mechanical behavior. Table 4 shows the mechanical properties of the developed samples.

The Young's modulus, indicating material stiffness, varied across the samples. P7B3 (70% PP and 30% PBR) showed a modulus of 820.7 MPa, while P7B3-10 and P7B3-20 (containing 10% and 20% PP-g-MA, respectively) exhibited slightly higher moduli of 832.5 MPa and 845.7 MPa. This increment suggests that the addition of PP-g-MA enhances the stiffness of the blend, likely due to improved interfacial adhesion between PP and PBR phases. Conversely, P6B4 (60%

Table 4. Mechanical properties of the developed samples.

Sample code	Young's modulus (MPa)	Ultimate tensile strength (MPa)	Elongation-at-break (%)
P7B3	820.7±8.7	24.2±1.9	430.8±9.4
P7B3-10	832.5±10.2	26.8±2.1	441.4±10.7
P7B3-20	845.7±7.9	28.2±2.7	457.5±12.2
P6B4	780.1±9.4	20.4±1.1	498.4±8.4
P6B4-10	791.6±8.4	23.4±1.5	520.4±8.7
P6B4-20	802.7±11.2	25.5±1.7	552.8±10.1

PP and 40% PBR) showed a lower modulus (780.1 MPa) compared to P7B3, which could be attributed to the higher rubber content leading to increased flexibility. The addition of PP-g-MA (P6B4-10 and P6B4-20) again increased the modulus to 791.6 MPa and 802.7 MPa, respectively, following the same trend observed in P7B3 blends.

The Ultimate Tensile Strength (UTS) followed a similar trend to the Young's modulus. P7B3 exhibited a UTS of 24.2 MPa, which increased with the addition of PP-g-MA (26.8 MPa for P7B3-10 and 28.2 MPa for P7B3-20). This increase can be linked to the enhanced compatibility and dispersion of the rubber phase in the PP matrix. P6B4 showed a lower UTS (20.4 MPa) compared to P7B3, supporting the idea that a higher rubber content results in lower tensile strength. However, the addition of PP-g-MA improved the UTS to 23.4 MPa and 25.5 MPa for P6B4-10 and P6B4-20, respectively.

P7B3 had an elongation-at-break of 430.8%, which slightly increased with the addition of PP-g-MA (441.4% for P7B3-10 and 457.5% for P7B3-20). This indicates that PP-g-MA not only improves stiffness and strength but also maintains or enhances the ductility of the blend. For the P6B4 series, the elongation-at-break was notably higher (498.4% for P6B4) than that of P7B3, reflecting the higher flexibility due to more rubber content. The elongation-at-break further increased with PP-g-MA addition (520.4% for P6B4-10 and 552.8% for P6B4-20), demonstrating the effectiveness of the compatibilizer in enhancing flexibility alongside mechanical strength.

CONCLUSION

In this study, thermoplastic vulcanizates were prepared based on PP/PBR at different blend compositions (70/30 and 60/40). The prepared TPVs demonstrated a non-uniform droplet-in-matrix morphology due to the coalescence of the rubber phase. This situation was more severe for the 60/40 composition, which was on the verge of forming a co-continuous morphology. To stabilize the blend structure and produce a more uniform morphology with finer PBR domains, we added PP-g-MA at different contents (10 and 20%) and studied its compatibilizing effects on the prepared TPVs. The SEM results revealed the compatibilizing effects of PP-g-MA in both contents for the 70/30 TPVs. However, only the 20% content of PP-g-MA exhibited a great compatibilizing effect for the 60/40 TPVs, due to the higher PBR content, which indicated a higher tendency for coalescence. Rheological results revealed a greatly enhanced elastic response for the 60/40 TPVs compared to the 70/30 TPVs, due to the higher PBR content. Viscoelastic response of the system was governed by two opposing effects; namely, the compatibilization effect of PP-g-MA, which increases the elastic response, and the PP-g-MA induced flowability, which increases the viscose response. It was found that the later effect dominates at higher PP-g-MA content, which proves the compatibilizing role of PP-g-MA. DMA results proved the existence of such opposing effects because the storage modulus values were distinctly governed by the former and later effects at low and high PP-g-MA contents, respectively. The impact strength values were also measured and correlated with other analyses. Results showed moderate and notable enhancements in the impact strength once low and high contents of PP-g-MA were used, respectively. The highly increased impact strength was attributed to the uniform and fine distribution of PBR domains within the PP matrix, facilitating the stress transfer from the plastic to the rubber phase.

CONFLICTS OF INTEREST

The authors declare that there is no conflict of interest.

REFERENCES

1. Ibrahim A, Dahlan M (1998) Thermoplastic natural rubber blends. Prog Polym Sci 23: 665–706
2. Ning N, Li S, Wu H, Tian H, Yao P, Guo-Hua HU, Tian M, Zhang L (2018). Preparation, microstructure, and microstructure-properties relationship of thermoplastic vulcanizates

(TPVs): A review. Prog Polym Sci 79: 61-97
3. Torabi A, Azadi F, Jafari SH, Khonakdar HA, Ruckdaschel H (2023) Correlation of morphology, rheology, thermal, and mechanical properties in PP/EOC blends in presence of nanoclay and compatibilizer. Polym-Plast Technol Mater 62: 1985-1997
4. De Sarkar M, Chandel N, Banerjee SS, Saha S, Bhowmick AK, Gupta S, Saroop M (2022) Development of high melt strength polypropylene and its application in thermoplastic elastomeric composition. J Elastomers Plast 54: 429–456
5. Entezam M, Nozari D, Mirjalili M, Khonakdar HA (2015) On the melt rheological behavior and microstructure of nanoclay-filled polyethylene/ethylene vinyl acetate (PE/EVA) blend. Polym-Plast Technol Eng 54: 1571-1584
6. Entezam M, Zarei I, Khonakdar HA (2022) Effect of accelerator solubility on the curing characteristics and physico-mechanical properties of SBR/NBR blends: correlation with feeding sequence and blend composition. Polym Bull 79: 1501–1519
7. Azizli MJ, Mokhtary M, Khonakdar HA, Goodarzi V (2020) Compatibilizer/graphene/carboxylated acrylonitrile butadiene rubber (XNBR)/ethylenepropylenediene monomer (EPDM) nanocomposites: Morphology, compatibility, rheology and mechanical properties. J Appl Polym Sci 137: app 49331
8. Hejazi I, Seyfi J, Sadeghi GM, Davachi SM (2011) Assessment of rheological and mechanical properties of nanostructured materials based on thermoplastic olefin blend and organoclay. Mater Des 32: 649-655
9. Bhattacharya AB, Raju AT, Chatterjee T, Naskar K (2020) Development and characterizations of ultra-high molecular weight EPDM/PP based TPV nanocomposites for automotive applications. Polym Compos 41: 4950-4962
10. Helal E, Pottier C, David E, Fréchette M, Demarquette NR (2018) Polyethylene/thermoplastic elastomer/Zinc Oxide nanocomposites for high voltage insulation applications: Dielectric, mechanical and rheological behavior. Eur Polym J 100: 258-269
11. Srivastava VK, Basak GC, Saha S, Rao GS, Jasra RV (2022) Epoxidized polybutadiene rubber as an effective compatibilizer for acrylonitrile butadiene rubber and polybutadiene rubber blend. J Elast Plast 54: 42-55
12. Wu B, Mao X, Wang C, Deng T, Li R, Xu Y, Tang X (2020) Different organic peroxides that cure low-k 1, 2-PB/SBS/EPDM composites for high-frequency substrate. J Vinyl Addit Technol 26: 524-535
13. Malas A, Pal P, Das CK (2014) Effect of expanded graphite and modified graphite flakes on the physical and thermo-mechanical properties of styrene butadiene rubber/polybutadiene rubber (SBR/BR) blends. Mater Des 55: 664–673
14. Ettelaie R, Murray BS, Liu S (2019) On the origin of seemingly nonsurface-active particles partitioning between phase-separated solutions of incompatible nonadsorbing polymers and their adsorption at the phase boundary. Langmuir 35: 9493–9503
15. Kiani F, Entezam M, Khonakdar HA, Jafari Sh, Callsen C, Altstädt V (2020) Assessment of compatibilization role of nanoclay in immiscible polystyrene/ethylene–octene copolymer blends via wide-angle X-ray scattering, microstructure, rheological analyses, and mechanical properties, J Appl Polym Sci 137: 48748
16. Entezam M, Poormadadkar H, Khonakdar HA, Jafari Sh (2020) Melt rheology and interfacial properties of binary and ternary blends of PS, EOC, and SEBS, J Appl Polym Sci 137: 48791
17. Seyni FI, Grady BP (2021) Janus particles as immiscible polymer blend compatibilizers: a review. Colloid Polym Sci 299: 585–593
18. Moeinifar E, Otadi M, Seyfi J, Khonakdar HA (2020) Study on the effects of polyhedral oligomeric silsesquioxane on compatibility, crystallization behavior and thermal stability of polylactic acid/polycaprolactone blends. Polym Bull 77: 585–598
19. Ebadi-Dehaghani H, Khonakdar HA, Barikani M, Jafari Sh, Wagenknecht U, Heinrich G (2016) An investigation on compatibilization threshold in the interface of polypropylene/polylactic acid blends using rheological studies, J Vinyl Addit Technol 22: 19-28
20. Saiwari S, Yusoh B, Thitithammawong A (2019) Recycled rubber from waste of natural rubber gloves blending with polypropylene for preparation of thermoplastic vulcanizates compatibilized by maleic anhydride. J Polym Environ 27: 1141–1149
21. Liu H, Liu X, Zhao F, Liu Y, Liu L, Wang L, Geng

C, Huang P (2020) Preparation of a hydrophilic and antibacterial dual function ultrafiltration membrane with quaternized graphene oxide as a modifier. J Colloid Interface Sci 562: 182-192
22. Moshkriz A, Darvishi R, Barati A, Askari M, Mosleh S (2021) Preparation and evaluation of thermoplastic vulcanizate/organo-modified layered double hydroxide nanocomposite: Statistical modelling and optimization. Mater Today Commun 26: 102046
23. Belhaoues A, Benmesli S, Riahi F (2020) Compatibilization of natural rubber–polypropylene thermoplastic elastomer blend. J Elast Plast 52: 728–746
24. Rafiei S, Soudbar D, Sadri M, Shafiei F (2022) Effects of compatibilizers on microstructural and viscoelastic properties of polypropylene/ polybutadiene thermoplastics vulcanizates. J Vinyl Addit Technol 28: 50–61
25. Sheng J, Qi LY, Yuan XB, Shen NX, Bian DC (1997) Blends of polypropylene with poly (cis-butadiene) rubber. I. Phase structure and morphology of blends. J Appl Polym Sci 64: 2265–2272
26. Saffari A, Sheikh A (2017) Peroxide dynamic crosslinking in impact modification of polypropylene with polybutadiene. Polym Test 57: 260–269
27. Khonakdar HA, Jafari SH, Wagenknecht U, Jehnichen D (2006) Effect of electron-irradiation on cross-link density and crystalline structure of low-and high-density polyethylene. Radiation physics and chemistry 75: 78-86
28. Mazidi MM, Aghjeh MKR, Khonakdar HA, Reuter U (2016) Structure–property relationships in super-toughened polypropylene-based ternary blends of core–shell morphology. Rsc Adv 6: 1508-1526
29. Mazidi MM, Sharifi H, Razavi-Aghjeh MK, Zare L, Khonakdar HA, Reuter U (2023) Super- tough PLA-based blends with excellent stiffness and greatly improved thermal resistance via interphase engineering. ACS Appl Mater Interfaces 15: 22445–22470
30. Khodabandelou M, Aghjeh MKR, Khonakdar HA, Mazidi MM (2017) Effect of localization of carbon nanotubes on fracture behavior of un-vulcanized and dynamically vulcanized PP/EPDM/MWCNT blend-nanocomposites. Compos Sci Technol 149: 134-148
31. Aghjeh MR, Mardani E, Rafiee F, Otadi M, Khonakdar HA, Jafari SH, Reuter U (2017) Analysis of dynamic oscillatory rheological properties of PP/EVA/organo-modified LDH ternary hybrids based on generalized Newtonian fluid and generalized linear viscoelastic approaches, Polym Bull 74: 465-482
32. Marcilla A, Garcia-Quesada JC, Hernandez J, Ruiz-Femenia R, Perez JM (2005) Study of polyethylene crosslinking with polybutadiene as coagent. Polym Test 24: 925-931
33. Ning N, Li S, Wu H, Tian H, Yao P, HU G, Tian M, Zhang L (2018) Preparation, microstructure, and microstructure-properties relationship of thermoplastic vulcanizates (TPVs): A review. Prog Polym Sci 79: 61-97
34. Zohrevand A, Goharpey F, Nasrollah Gavgani J, Foudazi R (2020) The effect of aggregation of cured rubber particles on rheology of thermoplastic vulcanizates. Polym Compos 41: 1376–1392
35. Caihong L, Ruijie X, Xiaogang L, Jiayi X (2018) Improving properties of dynamic vulcanized polyurethane and silicone rubber elastomer through controlling interphase layer. Polym-Plast Technol Eng 57: 1496–1505
36. Aghjeh MR, Khonakdar HA, Jafari SH, Zschech C, Gohs U, Heinrich G (2016), Rheological, morphological and mechanical investigations on ethylene octene copolymer toughened polypropylene prepared by continuous electron induced reactive processing, RSC Adv 6: 24651-24660
37. Aghdami RM, Mousavi SR, Estaji S, Dermeni RK, Khonakdar HA, Shakeri A (2022) Evaluating the mechanical, thermal, and antibacterial properties of poly (lactic acid)/silicone rubber blends reinforced with (3-aminopropyl) triethoxysilane-functionalized titanium dioxide nanoparticles. Polym Compos 43: 4165-4178
38. Gong Z, Fan J, Huang J, Yuan Z, Liu Y, Yuan D, Chen Y (2020) Toughening model of filled thermoplastic vulcanizates with dual-phase continuity. Mater Chem Phys 255: 123601
39. Ma LF, Wei XF, Zhang Q, Wang WK, Gu L, Yang W, Xie BH, Yang MB (2012) Toughening of polyamide 6 with β-nucleated thermoplastic vulcanizates based on polypropylene/ethylene–propylene–diene rubber grafted with maleic anhydride blends. Mater Des 33: 104-110